Stable and High Performance AlGaN Self-Aligned-Gate Field Emitter Arrays

Pao-Chuan Shih, *Graduate Student Member, IEEE*, Girish Rughoobur, Zachary Engel, Habib Ahmad, William Alan Doolittle, *Senior Member, IEEE*, Akintunde I. Akinwande, *Life Fellow, IEEE*, and Tomás Palacios, *Fellow, IEEE*

***Abstract*— AlGaN alloys are promising for field emission devices due to their low electron affinities. However, there have been limited demonstrations of AlGaN vacuum transistors so far. This letter combines a new self-aligned-gate (SAG) process and digital-etching tip sharpening to demonstrate three-terminal AlGaN SAG field emitter arrays (FEAs). These devices show a turn-on voltage of 19.5 V and an anode current density (J_A) of 100 mA/cm^2 at an overdrive voltage of 20 V, which are comparable with best Si devices. The AlGaN SAGFEAs can operate in DC mode at a fixed gate-emitter voltage (V_{GE}) with J_A of 3-5 mA/cm^2 for at least 5 hours without a significant degradation. The gate leakage does not increase after the long DC operation, suggesting high-performance and stable AlGaN vacuum transistors.**

***Index Terms*— AlGaN, field emission, vacuum transistor.**

I. Introduction

VACUUM devices are excellent candidates for harsh-environment and high-frequency electronics thanks to their radiation hardness and scattering-free electron transport [1]. Si and metal field emitters (FEs) have been developed into mature technologies in recent years [2]–[5]. III-Nitride semiconductors promise to further improve FEs thanks to their tunable electron affinities [6], [7]. With a lower electron affinity, electrons could tunnel from the semiconductor surface to vacuum more easily, leading to devices with a lower operating voltage. Ga-polar heavily-n-doped GaN self-aligned-gate field emitter arrays (SAGFEAs) have been demonstrated and improved with sharpened tips by wet-based digital etching (DE) recently [8], [9]. The gate-emitter turn-on voltage ($V_{GE,on}$) in these devices is comparable to the state-of-the-art Si devices, while the relatively low current density and device stability are still unsolved issues. Reference [8] observed that the gate insulator under the probing region breaks when V_{GE} approaches 50 V, while no damage was observed in the FEA region. Layout optimization is thus expected to improve device stability.

In addition to GaN, AlGaN alloys with high-Al ratio are expected to provide better performance than GaN because of reduced electron affinities [6]. However, most work on these materials has focused on two-terminal field emitters [10]–[13]. Very limited demonstrations of AlGaN three-terminal FEAs have been reported [14], [15], even though these devices are necessary for accurate benchmarking with other materials' systems. Schottky-diode-type electron emission devices based on the low electron affinities of AlGaN alloys have also been demonstrated; however, their power consumption is not competitive with the SAGFEAs [16], [17]. In this work, we have fabricated AlGaN SAGFEAs with a similar SAG geometry and DE recently demonstrated for GaN SAGFEAs [8], [9]. We show a clear performance improvement, compared to simultaneously-fabricated GaN devices. For these AlGaN SAGFEAs, a turn on voltages ($V_{GE,on}$) of 19-22 V and anode current densities (J_A) approaching 100 mA/cm^2 at an overdrive voltage ($V_{OV} = V_{GE} - V_{GE,on}$) of 20 V were demonstrated, which are similar to the best Si devices. Additionally, these AlGaN SAGFEAs show over 5 hours of stable DC operation for anode current density (J_A) of 3-5 mA/cm^2 with no increase of gate leakage. These results show the great potential for III-Nitride devices to outperform Si devices in the future.

II. Device Fabrication

Baseline GaN SAGFEAs are fabricated on a GaN-on-Si wafer grown by Enkris Semiconductor, Inc. by metal organic chemical vapor deposition (MOCVD) [8]. The structure consists of a 1.4 μm n^{++}-GaN (Si: 1 $\times$ 10^{19} cm^{-3}) layer on a 1.4 μm buffer layer grown on the Si substrate. AlGaN SAGFEAs are fabricated on a 1 cm$\times$1 cm coupon grown at the Georgia Institute of Technology. This AlGaN material consists of a 420-nm n$^+$ AlGaN layer and a 200-nm non-intentionally-doped AlN layer, which are grown by molecular beam epitaxy (MBE), on a commercial AlN template [18]–[20]. The AlN template is grown on the sapphire substrate via hydride vapor phase epitaxy (HVPE). The Al composition in this AlGaN

Manuscript received 25 May 2022; revised 15 June 2022; accepted 18 June 2022. Date of publication 21 June 2022; date of current version 26 July 2022. This work was supported by the Air Force Office of Scientific Research (AFOSR) through the Multidisciplinary Research Program of the University Research Initiative (MURI), under Grant FA9550-18-1-0436. The review of this letter was arranged by Editor R. Xiao. *(Corresponding authors: Pao-Chuan Shih; Tomás Palacios.)*

Pao-Chuan Shih, Girish Rughoobur, Akintunde I. Akinwande, and Tomás Palacios are with the Microsystems Technology Laboratories, Massachusetts Institute of Technology, Cambridge, MA 02139 USA (e-mail: pcshih@mit.edu; tpalacios@mit.edu).

Zachary Engel, Habib Ahmad, and William Alan Doolittle are with the School of Electrical and Computer Engineering, Georgia Institute of Technology, Atlanta, GA 30332 USA.

Color versions of one or more figures in this letter are available at https://doi.org/10.1109/LED.2022.3184996.

Digital Object Identifier 10.1109/LED.2022.3184996

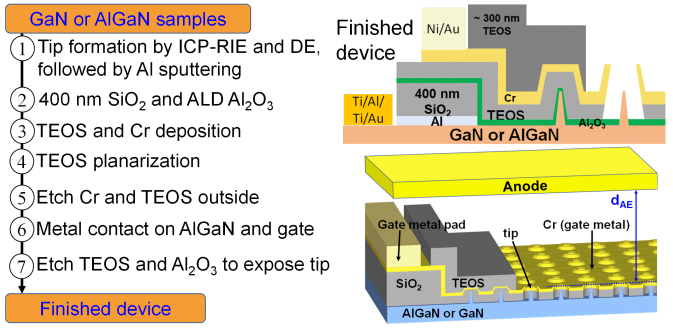

Fig. 1. Process flow, geometry of the finished device, and 3D image of the measurement setup featuring an anode electrode suspended on top of the SAGFEA. The anode-emitter distance (d_{AE}) is fixed at about 2 mm in all measurements.

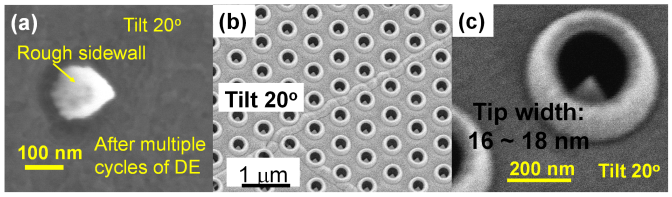

Fig. 2. Tilted SEM images of (a) an AlGaN tip after DE, (b) large-area and (c) zoom-in SEM images of a finished AlGaN FEA. Compared to GaN tips, the sidewall of AlGaN tips after DE is rough [9].

material is 37.6%, as measured by x-ray diffraction (XRD). The Hall electron concentration of the n^+ AlGaN layer is about 3.9×10^{19} cm^{-3}.

Fig. 1(a) shows the fabrication process flow, and the details of different processing steps can be found in prior work [8]. The III-N tips are firstly formed by dry etching and are then sharpened by DE to obtain sub-20 nm tip width [9]. Contrary to GaN, it is observed that the AlGaN sidewalls become rough after DE (Fig. 2(a)). The rough sidewalls can potentially provide additional electron emission sites and increase gate leakage. After tip formation, an additional 400-nm plasma enhanced chemical vapor deposition (PECVD) SiO_2 is added with respect to our prior work in [8] to prevent early breakdown happening under the gate pad. A 10-nm Al_2O_3 is then deposited by atomic layer deposition (ALD) to protect III-N tips from subsequent plasma dry etching. In the last step, tips are exposed by a two-step etching. The tetraethyl orthosilicate (TEOS) is firstly etched by timed dry etching, and the Al_2O_3 and residual TEOS are then etched by shortly dipping the sample in buffer oxide etchant (BOE). The scanning electron microscopy (SEM) images of a finished AlGaN FEA with sub-20-nm tip width are shown in Fig. 2(b) and (c).

III. Results and Discussion

After SEM inspection, samples are loaded into a ultra-high vacuum (UHV) system for measurement at a base pressure of 1-2 $\times 10^{-9}$ Torr. The anode is a suspended 0.5-mm-diameter tungsten ball which can be moved to position on top of the measured FEA. The anode-emitter distance (d_{AE}) is kept around 2 mm in all measurements in this work.

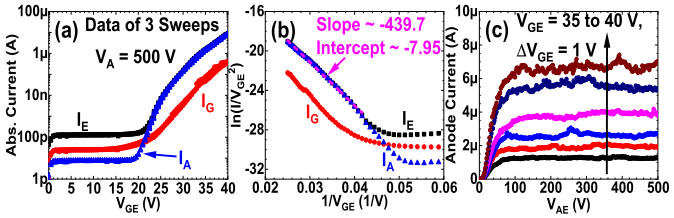

Fig. 3. (a) Transfer characteristics, (b) corresponding Fowler-Nordheim plot, and (c) output characteristics of one of the best AlGaN FEAs. This FEA consists of 150 × 150 tips.

The transfer and output characteristics after proper conditioning of one of the best AlGaN SAGEFAs are shown in Fig. 3. This AlGaN FEA consists of 150 × 150 tips, and the FEA area is about 96 μm × 80 μm. The transfer characteristics are stable as there is no clear deviation between 3 sequential measurements. The device turns on at a gate-emitter voltage (V_{GE}) of 19.5 V at which point the anode current (I_A) increases to 10 pA from the noise level. The maximum anode current is 8 μA, which corresponds to a current density J_A of about 100 mA/cm^2. Moreover, though the AlGaN sidewalls are rough after DE (Fig. 2(a)), the gate leakage (I_G) is still at least one-order-of-magnitude lower than the anode current. The Fowler-Nordheim (F-N) plot of I_A shows a clear straight line with a slope ($-b_{FN}$) of -439.7 (V) (Fig. 3(b)). The output characteristics of this AlGaN device shows a stable anode current for anode-emitter voltages (V_{AE}) above 100 V. This large V_{AE} is due to space-charge limit (Child's law) [21], [22], and it can be reduced by integrating the anode into the device structure and reducing, in that way, the anode-emitter distance, d_{AE} [23]. The device is stable and I_G does not increase after the measurements.

A different AlGaN SAGFEA with 150 × 150 tips is measured for both transfer characteristics and DC operation lifetime (Fig. 4). Based on the transfer characteristics (Fig. 4(a)), the device does not show significant degradation after a total 5-hr DC operation at a fixed V_{GE} of 37 V (Fig. 4(b)). At the beginning of the lifetime test, I_A was about 400 nA, which corresponds to a current density J_A of about 5 mA/cm^2. Both I_A and I_G gradually decrease during the lifetime test, and the measurement stops when the I_A goes below 200 nA. F-N parameters for multiple transfer characteristics before and after lifetime test are plotted in the Seppen-Katamuki (S-K) chart (Fig. 4(c)). As the data points stay in the same region of the S-K chart, it is clear that the device does not degrade significantly [24]. The variability during the lifetime measurement could be related to noise introduced by micro-vibrations happening during the measurement, as the anode is a suspended metal ball in the measurement system, which is not fixed to the device.

The F-N parameters of 4 different AlGaN SAGFEAs and a baseline GaN device fabricated through the same process are summarized and compared with our prior work in the S-K chart shown in Fig. 5(a). Low $|b_{FN}|$ and large $ln(a_{FN})$ are desired for lower operating voltage and higher anode current. Although the performance of the baseline GaN device is slightly worse than prior work [8], the changes in device

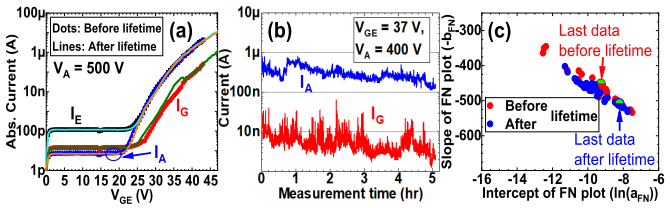

Fig. 4. (a) Transfer characteristics before and after lifetime test, (b) lifetime test, and (c) Seppen-Katamuki (S-K) chart of an AlGaN FEA. This FEA consists of 150 × 150 tips. Anode current of 1 μA is equal to about 13 mA/cm^2.

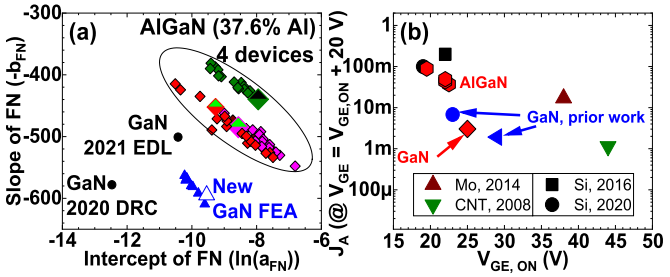

Fig. 5. (a) S-K chart of fabricated III-N self-align-gated FEAs and (b) benchmark of different materials FEAs [3], [4], [8], [26]–[28]. The same-color labels in (a) represent F-N parameters of different transfer characteristics from one FEA after conditioning. The red labels in (b) represent devices in this work.

fabrication allow the new GaN device to be more stable than the one in reference [8], and the early breakdown in the insulator layer under the probing region is eliminated. Furthermore, the AlGaN devices clearly show better performance than GaN devices thanks to their potentially-lower work function. The effective work function is typically lower if the data points are located at a more upper-right region in the S-K chart [24]. Ideally, heavily doped n-type AlGaN alloy with a higher Al composition ratio should provide better performance because of a lower electron affinity. However, surface states, doping activation energies, and defects, which are generated during growth and device fabrication, are related to the Al composition ratio and will affect the surface effective work function of the fabricated tips [9], [25]. Moreover, high-Al-composition AlGaN materials are prone to form oxide in air, which will also change the energy barriers for electron field emission. Therefore, there might be an optimum Al composition ratio of the AlGaN alloy for the field emission devices, while it still requires more detailed study on different aspects mentioned above.

The III-N SAGFEAs demonstrated in this work are also compared with SAGFEAs based on other materials (Fig. 5(b)) [3], [4], [8], [26]–[28]. When setting an overdrive voltage (V_{OV} = V_{GE} - $V_{GE,ON}$) of 20 V, the J_A of our AlGaN SAGFEAs approaches 100 mA/cm^2 and is comparable with state-of-the-art Si SAGFEAs. Based on the F-N parameter (b_{FN} = 439.7 V), our AlGaN SAGFEAs can potentially outperform Si devices. However, the defects introduced in the AlGaN devices by the dry etching and DE (Fig. 2(a) and (b)) make these devices prone to break at higher V_{GE}. A strong electric field at high V_{GE} in the oxide layer covering the unexposed tips (as shown in the cross-section geometry in Fig. 1) can also cause gate oxide breakdown. These unexposed tips are necessary to extend out the gate metal from the FEA region to the gate pad region, and further optimization is necessary to mitigate or eliminate this failure mechanism. With further optimization on different etching process and device geometry, the device is expected to be more stable and to be able to support a higher gate voltage. More detailed study on device stability and lifetime at different current densities can then be done for better III-N SAGFEAs in the future.

IV. Conclusion

Three-terminal 37.6%-Al AlGaN SAGFEAs are demonstrated with a turn-on voltage of 19.5 V at I_A = 10 pA and a J_A of 100 mA/cm^2 at V_{GE} = 40 V. Thanks to the lower effective work function, the operation voltage and current density of AlGaN SAGFEAs are better than GaN devices, and competitive with state-of-the-art Si devices. These AlGaN SAGFEAs can operate in DC mode with J_A of 3-5 mA/cm^2 at a fixed V_{GE} for 5 hours without a clear degradation, suggesting stable field emission devices. Though further study on material properties and fabrication optimization is needed, these results show that AlGaN SAGFEAs have great potential for high-frequency and harsh-environment applications.

Acknowledgment

The GaN-on-Si coupon used in this work was obtained from the same 6-inch wafer reported in prior work [8], provided by Enkris, Inc. The AlGaN materials were grown by MBE on AlN templates and characterized at the Georgia Institute of Technology. The device fabrication and characterization was conducted in MTL, NSL, and MIT.nano at MIT.

References

[1] J.-W. Han, J. S. Oh, and M. Meyyappan, "Vacuum nanoelectronics: Back to the future?—Gate insulated nanoscale vacuum channel transistor," *Appl. Phys. Lett.*, vol. 100, May 2012, Art. no. 213505, doi: 10.1063/1.4717751.

[2] Y. Neo, T. Soda, M. Takeda, M. Nagao, T. Yoshida, C. Yasumuro, S. Kanemaru, T. Sakai, K. Hagiwara, N. Saito, T. Aoki, and H. Mimura, "Focusing characteristics of double-gated field-emitter arrays with a lower height of the focusing electrode," *Appl. Phys. Exp.*, vol. 1, May 2008, Art. no. 053001, doi: 10.1143/APEX.1.053001.

[3] S. A. Guerrera and A. I. Akinwande, "Silicon field emitter arrays with current densities exceeding 100 A/cm^2 at gate voltages below 75 V," *IEEE Electron Device Lett.*, vol. 37, no. 1, pp. 96–99, Jan. 2016, doi: 10.1109/LED.2015.2499440.

[4] N. Karaulac, G. Rughoobur, and A. I. Akinwande, "Highly uniform silicon field emitter arrays fabricated using a trilevel resist process," *J. Vac. Sci. Technol. B, Microelectron.*, vol. 38, no. 2, Mar. 2020, Art. no. 023201, doi: 10.1116/1.5131656.

[5] C. A. Spindt, I. Brodie, L. Humphrey, and E. R. Westerberg, "Physical properties of thin-film field emission cathodes with molybdenum cones," *J. Appl. Phys.*, vol. 47, no. 12, pp. 5248–5263, Dec. 1976, doi: 10.1063/1.322600.

[6] S. P. Grabowski, M. Schneider, H. Nienhaus, and W. Mönch, "Electron affinity of $Al_xGa_{1-x}N$(0001) surfaces," *Appl. Phys. Lett.*, vol. 78, no. 17, pp. 2503–2505, 2001, doi: 10.1063/1.1367275.

[7] S.-C. Lin, C. T. Kuo, X. Liu, L. Y. Liang, and C. H. Cheng, "Experimental determination of electron affinities for InN and GaN polar surfaces," *Appl. Phys. Exp.*, vol. 5, Mar. 2012, Art. no. 031003, doi: 10.1143/APEX.5.031003.

[8] P.C. Shih, G. Rughoobur, K. Chang, A.I. Akinwande, and T. Palacios, "Self-align-gated GaN field emitter arrays sharpened by a digital etching process," *IEEE Electron Device Lett.*, vol. 42, no. 3, pp. 422–425, Mar. 2021, doi: 10.1109/LED.2021.3052715.

[9] P.-C. Shih, Z. Engel, H. Ahmad, W. A. Doolittle, and T. Palacios, "Wet-based digital etching on GaN and AlGaN," *Appl. Phys. Lett.*, vol. 120, no. 2, Jan. 2022, Art. no. 022101, doi: 10.1063/5.0074443.

[10] M. Kasu and N. Kobayashi, "Field-emission characteristics and large current density of heavily Si-doped AlN and $Al_xGa_{1-x}N$ ($0.38 \leq x < 1$)," *Appl. Phys. Lett.*, vol. 79, no. 22, pp. 3642–3644, 2001, doi: 10.1063/1.1421223.

[11] S.-C. Shi, C.-F. Chen, S. Chattopadhyay, K.-H. Chen, and L.-C. Chen, "Field emission from quasi-aligned aluminum nitride nanotips," *Appl. Phys. Lett.*, vol. 87, no. 7, Aug. 2005, Art. no. 073109, doi: 10.1063/1.2009838.

[12] A. Evtukh, O. Yilmazoglu, V. Litovchenko, M. Semenenko, T. Gorbanyuk, A. Grygoriev, H. Hartnagel, and D. Pavlidis, "Electron field emission from nanostructured surfaces of GaN and AlGaN," *Phys. Status Solidi C*, vol. 5, no. 2, pp. 425–430, Feb. 2008, doi: 10.1002/pssc.200777450.

[13] F. Giubileo, A. D. Bartolomeo, Y. Zhong, S. Zhao, and M. Passacantando, "Field emission from AlGaN nanowires with low turn-on field," *Nanotechnology*, vol. 31, no. 47, Nov. 2020, Art. no. 475702, doi: 10.1088/1361-6528/abaf22.

[14] T. Kozawa, T. Ohwaki, Y. Taga, and N. Sawaki, "Field emission study of gated GaN and $Al_{0.1}Ga_{0.9}N$/GaN pyramidal field emitter arrays," *Appl. Phys. Lett.*, vol. 75, no. 21, pp. 3330–3332, 1999, doi: 10.1063/1.125341.

[15] Y. Taniyasu, M. Kasu, and T. Makimoto, "Field emission properties of heavily Si-doped AlN in triode-type display structure," *Appl. Phys. Lett.*, vol. 84, no. 12, pp. 2115–2117, Mar. 2004, doi: 10.1063/1.1689398.

[16] M. Deguchi and T. Uenoyama, "Electron emission from graded $Al_xGa_{1-x}N$/GaN negative-electron-affinity cold cathodes," *Jpn. J. Appl. Phys.*, vol. 39, no. 7A, pp. L641–L643, 2000, doi: 10.1143/JJAP.39.L641.

[17] R. Pillai, D. Starikov, C. Boney, and A. Bensaoula, "Hardened planar nitride based cold cathode electron emitter," *Proc. SPIE*, vol. 8262, Feb. 2012, Art. no. 82620O, doi: 10.1117/12.909587.

[18] E. A. Clinton, Z. Engel, E. Vadiee, J. V. Carpenter, Z. C. Holman, and W. A. Doolittle, "Ultra-wide-bandgap AlGaN homojunction tunnel diodes with negative differential resistance," *Appl. Phys. Lett.*, vol. 115, no. 8, Aug. 2019, Art. no. 082104, doi: 10.1063/1.5113503.

[19] Z. Engel, E. A. Clinton, K. Motoki, H. Ahmad, C. M. Matthews, and W. A. Doolittle, "Adlayer control for tunable AlGaN self-assembled superlattices," *J. Appl. Phys.*, vol. 130, no. 16, Oct. 2021, Art. no. 165304, doi: 10.1063/5.0069534.

[20] H. Ahmad, Z. Engel, C. M. Matthews, S. Lee, and W. A. Doolittle, "Realization of homojunction PN AlN diodes," *J. Appl. Phys.*, vol. 131, no. 17, May 2022, Art. no. 175701, doi: 10.1063/5.0086314.

[21] K. L. Jensen, M. A. Kodis, R. A. Murphy, and E. G. Zaidman, "Space charge effects on the current-voltage characteristics of gated field emitter arrays," *J. Appl. Phys.*, vol. 82, no. 2, pp. 845–854, Jul. 1997, doi: 10.1063/1.365783.

[22] G. N. A. van Veen, "Space-charge effects in Spindt-type field emission cathodes," *J. Vac. Sci. Technol. B, Microelectron.*, vol. 12, no. 2, pp. 655–661, 1994, doi: 10.1116/1.587407.

[23] J.-W. Han, M.-L. Seol, D.-I. Moon, G. Hunter, and M. Meyyappan, "Nanoscale vacuum channel transistors fabricated on silicon carbide wafers," *Nature Electron.*, vol. 2, no. 9, pp. 405–411, Sep. 2019, doi: 10.1038/s41928-019-0289-z.

[24] Y. Gotoh, M. Nagao, D. Nozaki, K. Utsumi, K. Inoue, T. Nakatani, T. Sakashita, K. Betsui, H. Tsuji, and J. Ishikawa, "Electron emission properties of spindt-type platinum field emission cathodes," *J. Appl. Phys.*, vol. 95, no. 3, pp. 1537–1549, Feb. 2004, doi: 10.1063/1.1635655.

[25] B. S. Eller, J. Yang, and R. J. Nemanich, "Polarization effects of GaN and AlGaN: Polarization bound charge, band bending, and electronic surface states," *J. Electron. Mater.*, vol. 43, no. 12, pp. 4560–4568, Dec. 2014, doi: 10.1007/s11664-014-3383-z.

[26] A. Mustonen, V. Guzenko, C. Spreu, T. Feurer, and S. Tsujino, "High-density metallic nano-emitter arrays and their field emission characteristics," *Nanotechnology*, vol. 25, no. 8, Feb. 2014, Art. no. 085203, doi: 10.1088/0957-4484/25/8/085203.

[27] J. L. Davidson, W. P. Kang, K. Subramanian, and Y. M. Wong, "Vacuum cold cathode emitter electronic devices comprised of diamond or other carbons," in *Proc. UGIM*, 2008, pp. 102–106, doi: 10.1109/UGIM.2008.33.

[28] P.-C. Shih, G. Rughoobur, P. Xiang, K. Liu, K. Cheng, A. I. Akinwande, and T. Palacios, "GaN nanowire field emitters with a self-aligned gate process," in *Proc. Device Res. Conf. (DRC)*, Jun. 2020, pp. 1–2, doi: 10.1109/DRC50226.2020.9135161.